Rapid Echo Simulation for One-stationary Bistatic SAR Based on FFT and Subaperture Processing

Hongtu Xie, Daoxiang An, Xiaotao Huang, and Zhimin Zhou
College of Electronic Science and Engineering, National University of Defense Technology
Changsha, Hunan 410073, China

Abstract— In this study, a rapid echo simulation method based on fast Fourier transform (FFT) and subaperture processing for the one-stationary bistatic synthetic aperture radar (OSBSAR) is presented. First, the OSBSAR geometry is built in elliptical polar coordinate, and then the scene is divided into several equidistant elliptical rings. Based on the equivalent scatterer model, the approximate SAR system transfer function is derived, thus each pulse echo is calculated by the convolution of the transmitted signal and transfer function using the FFT. To further improve the simulation efficiency, the subaperture and subscene processing are used. The transfer function for the same subaperture pulses is calculated by the weighted sum of all the subscene equivalent scattering coefficient in the same equidistant elliptical ring using the FFT. Implementation of the proposed method is discussed. Simulation results are given to prove its validity.

1. INTRODUCTION

One-stationary bistatic synthetic aperture radar (OSBSAR) [1] is a special bistatic SAR (BSAR) system [2], with a stationary radar fixed on the top of a high tower or mountain. It inherits the BSAR advantages, such as greater anti-jamming ability, reducing military vulnerability, getting additional information and flexibility of the system design. Therefore, it has gained wide attention in both military and civilian fields [3].

Echo simulation is important in the SAR research, such as the system design, algorithms test and so on [4]. In general, the echo simulation contains the scene simulation and rapid echo generation. The simulation of the BSAR scene scattering characteristic was studied in [5]. In this paper, we only focus on the rapid generation of the OSBSAR echo, which means that we start with a reflectivity map as an input.

Echo simulation methods main include the time-domain method, two dimensional FFT (2DFFT) method and imaging inverse processing (IMIP) method. Time-domain method simulates echo data pulse by pulse and target by target (TBT) according to the SAR geometry. It can simulate the accuracy echo because of no approximation, but with the huge computational load. 2DFFT method [6] and IMIP method [7] has the high simulation efficiency but with some approximate processing in the echo simulaton. To improve the simulation efficiency but with the high simulation precision, a subaperture based echo simulation method for monstatic SAR is given in [8], which may be extend for the BSAR echo simulation.

This paper explores a rapid echo simulation (RES) method for OSBSAR based on [8]. Section 2 introduces the echo simulation based on equivalent scatterer. Section 3 describes the proposed RES method for OSBSAR in detail Section 4 proves its validity based on the simulation results. Section 5 gives the conclusion.

2. ECHO SIMULATION BASED ON EQUIVALENT SCATTERER

OSBSAR geometry is shown in Fig. 1. Moving radar moves parallel to Y axis direction, with the position $(0, y_M(\eta), z_M)$ at the slow time η. Stationary radar is located at $(x_S, 0, z_S)$. The scene is composed of several targets distributed on rectangle grids. Scene grid size is $M \times N$ (range $\times$ azimuth), and the range and azimuth spacing between adjacent grids are Δx and Δy, respectively. $x_{\min}$ is the minimum ground range of the scene, and its azimuth center line is the X axis. Assume that the moving and stationary radars of OSBSAR are perfectly synchronized. The bistatic range from the moving and stationary radars to the grid (m, n) at η is

$$\begin{aligned} R(\eta, m, n) &= R_M(\eta, m, n) + R_S(\eta, m, n) \\ &= \sqrt{(x_{\min} + m\Delta x)^2 + (y_M(\eta) - (n - N/2)\Delta y)^2 + z_M^2} \\ &\quad + \sqrt{(x_S - (x_{\min} + m\Delta x))^2 + ((n - N/2)\Delta y)^2 + z_S^2},\ 1 \le m \le M,\ 1 \le n \le N \quad (1) \end{aligned}$$

Supposed that the transmitted signal is $p(\tau) = w_r(\tau)\exp(j2\pi f_c\tau + j\pi\gamma\tau^2)$. τ is the fast time, γ is the chirp rate, $w_r(\cdot)$ is the range envelope, c is the speed of light, f_c is the center frequency. Thus the scene echo is

$$s(\tau,\eta) = \sum_{m=1}^{M}\sum_{n=1}^{N}\sigma_{mn}w_r\left[\tau - R(\eta,m,n)/c\right]\cdot\exp\left[-j2\pi f_c R(\eta,m,n)/c + j\pi\gamma\left(\tau - R(\eta,m,n)/c\right)^2\right] \tag{2}$$

where σ_{mn} is the scattering coefficient of the grid (m,n).

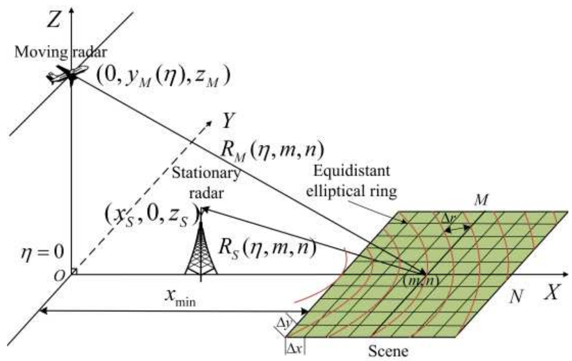

Figure 1: Imaging geometry of the OSBSAR.

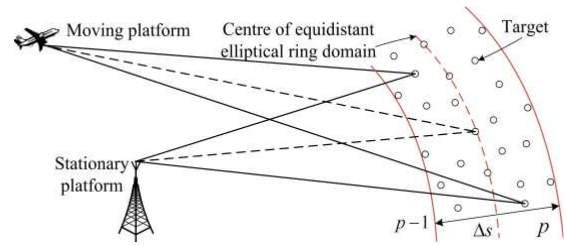

Figure 2: Target distribution between two adjacent equidistant elliptical rings.

To improve the speed, the fast echo simulation based on the equivalent scatterer is first introduced. Basic idea is to divide the scene into several equidistant elliptical rings, and the targets in scene are considered as distributing in the equidistant elliptical rings. The scattering coefficient of targets in the same equidistant elliptical ring is substituted by that of an equivalent scatterer. Assume that Δs is the interval between the adjacent elliptical rings. $R_{\min}(\eta)$ and $R_{\max}(\eta)$ are minimum and maximum ranges from the moving and stationary radars to the scene. The number of equidistant elliptical rings is

$$N_p(\eta) = round((R_{\max}(\eta) - R_{\min}(\eta))/\Delta s) + 1 \tag{3}$$

The target distribution between two adjacent equidistant elliptical rings is shown in Fig. 2. $p-1$ and p are two adjacent equidistant elliptical rings, and the bistatic ranges from them to the radars are $R_{\min}(\eta) + (p-1)\Delta s$ and $R_{\min}(\eta) + p\Delta s$, respectively. The spacing between the $(p-1)$-th and p-th equidistant elliptical rings is the p-th equidistant elliptical ring domain. The dashed ring is its center, and the bistatic range from it to the radars is

$$R(\eta,p) = R_{\min}(\eta) + (p-1/2)\Delta s \tag{4}$$

To calculate targets' scattering coefficients in the center of the equidistant elliptical ring domain, the bistatic ranges from the radars to all targets in this domain is replaced by the bistatic range from the radars to its center. So, an equivalent scatterer is substituted for all targets in this domain, whose scattering coefficient is

$$\sigma(\eta,p) = \sum_{i=1}^{I_p}\sigma_i\exp\left[-j2\pi f_c\Delta R_i(\eta,p)/c\right] \tag{5}$$

I_p is the number of targets in the p-th equidistant elliptical ring domain, σ_i is the i-th target's scattering coefficient. $\Delta R_i(\eta,p)$ is the difference between the bistatic range from the i-th target to the radars and bistatic range from the center of the p-th equidistant elliptical ring domain to the radars, then we have

$$\Delta R_i(\eta,p) = R_i(\eta) - (R_{\min}(\eta) + (p-1/2)\Delta s) \tag{6}$$

Based on the equivalent scatterer, the scene echo is rewritten as

$$s(\tau,\eta) = \sum_{p=1}^{N_p(\eta)}\sigma(\eta,p)\exp\left[-j2\pi f_c R(\eta,p)/c\right]\cdot w_r\left[\tau - R(\eta,p)/c\right]\exp\left[j\pi\gamma\left(\tau - R(\eta,p)/c\right)^2\right] \tag{7}$$

We can find that the latter two items in (7) are only related to τ. So, the scene echo can be rewritten as

$$s(\tau,\eta)=w_r(\tau)\exp(j\pi\gamma\tau^2)\otimes_\tau\sum_{p=1}^{N_p(\eta)}\sigma(\eta,p)\exp\left[-j2\pi f_c R(\eta,p)/c\right]\cdot\delta\left[\tau-R(\eta,p)/c\right]\tag{8}$$

$\otimes_\tau$ is the convolution versus τ. It is well known that the convolution can be performed by the FFT.

3. RES FOR OSBSAR

To further improve the simulation speed, the subaperture and subscene processing is used. First, the system transfer function for the same subaperture pulses is calculated by the weighted sum of all the subscenes equivalent scattering coefficient in the same equidistant elliptical ring domain, and then the subaperture pulse echo is simulated by the convolution of the transmitted signal and system transfer function using the FFT.

3.1. Geometry in Elliptical Polar Coordinate

Geometry in elliptical polar coordinate is shown in Fig. 3. A_{η_c} is the moving radar position at the aperture center time η_c, and A_η is the moving radar position at η. B is the stationary radar position. The position of the arbitrary scene grid (m,n) is $(x_m,y_n,0)$. The range between the grid (m,n) and A_{η_c} is r_M, and r_S is the range from the grid (m,n) to B. Let ρ be the bistatic range of the grid(m,n) and θ be the angle between r_M and Y axis positive direction at η_c, respectively. $\Delta\theta$ is the angular sampling spacing of the scene. So the elliptical polar coordinates of the grid (m,n) are defined as follow

$$\begin{cases}\rho=r_M+r_S=R_M(\eta_c,m,n)+R_S(\eta_c,m,n)\\ \theta=\arccos\left((y_n-y_M(\eta_c))/r_M\right),\theta\in\left[(\pi-\Theta)/2,(\pi+\Theta)/2\right]\end{cases}\tag{9}$$

Θ is the moving radar beam width. As shown in [1], r_M and r_S can be expressed as a function of (ρ,θ).

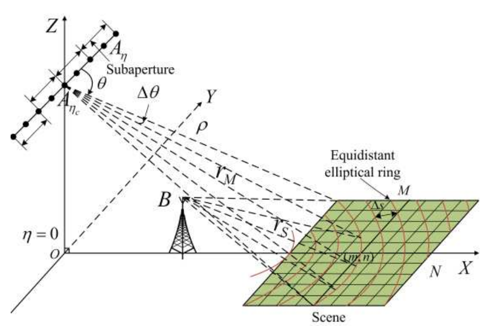

Figure 3: Geometry in elliptical polar coordinate.

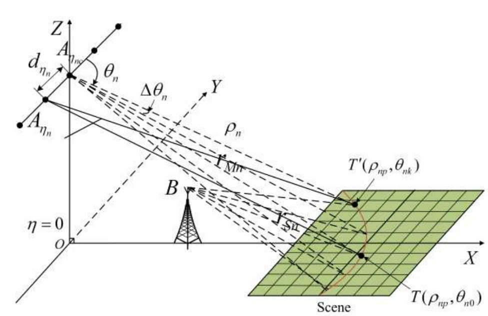

Figure 4: Subaperture processing in the echo simulation.

In Fig. 3, the scene is divided into several elliptical polar subscenes, and the targets in scene is considered as distributing in the elliptical polar subscenes. $R(\eta,\rho_p,\theta_k)$ is the bistatic range from the A_η and B to the k-th elliptical polar subscene in the p-th equidistant elliptical ring domain. Thus, the scene echo is given by

$$s(\tau,\eta)=w_r(\tau)\exp(j\pi\gamma\tau^2)\otimes_\tau\sum_{p=1}^{N_p(\eta)}\sum_{k=1}^{N_k(\eta)}\sigma(\eta,\rho_p,\theta_k)\cdot\exp\left[-j2\pi f_c R(\eta,\rho_p,\theta_k)/c\right]\cdot\delta\left[\tau-R(\eta,\rho_p,\theta_k)/c\right]\tag{10}$$

where $N_k(\eta)$ is the number of the elliptical polar subscenes in the p-th equidistant elliptical ring domain at η. $\sigma(\eta,\rho_p,\theta_k)$ is the scattering coefficient of the k-th elliptical polar subscene in this domain, which is

$$\sigma(\eta,\rho_p,\theta_k)=\sum_{i=1}^{I_{p,k}}\sigma_i\exp\left[-j2\pi f_c\left(R_i(\eta)-R(\eta,\rho_p,\theta_k)\right)/c\right]\tag{11}$$

$I_{p,k}$ is the number of targets in the k-th elliptical subscene in the p-th equidistant elliptical ring domain.

3.2. Subaperture Processing

Radar pulses are split into several groups, i.e., subapertures (See Fig. 3). Each subaperture contains the same number of radar pulses. Assume that the subaperture time is very short, so all pulses in the same subaperture is considered as sharing the same scene scope [8]. Subaperture processing in the echo simulation is shown in Fig. 4. Suppose that η_{nc} is the n-th subaperture center time, $A_{\eta_{nc}}$ is the radar position of the central pulse at η_{nc}, A_{η_n} is the radar current position at η_n. The elliptical polar coordinates (ρ_n, θ_n) are defined similar to (ρ, θ) in Fig. 3. $\Delta\theta_n$ is the scene angular sampling spacing. d_{η_n} is the length of $\overline{A_{\eta_{nc}} A_{\eta_n}}$. $T'(\rho_{np}, \theta_{nk})$ and $T(\rho_{np}, \theta_{n0})$ are two elliptical subscenes in the p-th equidistant elliptical ring domain, and $\theta_{nk} = \theta_{n0} + k\Delta\theta_n$. Considering the central pulse position $A_{\eta_{nc}}$, the range $R(\eta, \rho_p, \theta_k)$ in (10) is the same for all elliptical subscenes in the p-th equidistant elliptical ring domain. Thus, (10) can become

$$\begin{aligned} s(\tau, \eta_{nc}) \;=\; & w_r(\tau)\exp(j\pi\gamma\tau^2) \otimes_\tau \sum_{p=1}^{N_p(\eta_{nc})} \sum_{k=-N_k(\eta_{nc})/2}^{N_k(\eta_{nc})/2} \sigma(\eta_{nc}, \rho_{np}, \theta_{nk}) \\ & \cdot \exp\left[-j2\pi f_c R(\eta_{nc}, \rho_{np})/c\right] \cdot \delta\left[\tau - R(\eta_{nc}, \rho_{np})/c\right] \end{aligned} \tag{12}$$

$R(\eta_{nc}, \rho_{np})$ is the bistatic range from radars $A_{\eta_{nc}}$ and B to the p-th elliptical ring domain. As considering other pulse position A_{η_n}, the bistatic range $R(\eta_n, \rho_{np}, \theta_{nk})$ is different from the bistatic range $R(\eta_{nc}, \rho_{np})$. But $R(\eta_n, \rho_{np}, \theta_{nk})$ can be computed from $R(\eta_{nc}, \rho_{np})$. Thus, we have

$$\begin{aligned} R(\eta_n, \rho_{np}, \theta_{nk}) \;=\; & |A_{n\eta}T'| + |BT'| = \left(|A_{nc}T'| + |BT'|\right) + \left[\left(|A_{n\eta}T'| + |BT'|\right) - \left(|A_{n\eta}T| + |BT|\right)\right] \\ & + \left(|A_{n\eta}T| - |A_{nc}T|\right) = R(\eta_{nc}, \rho_{np}) + \Delta R_1 + \Delta R_2 \end{aligned} \tag{13}$$

From (13), we can find that the ranges $R(\eta_{nc}, \rho_{np})$ and ΔR_2 is independent of k. Thus, (10) can be written as

$$\begin{aligned} s(\tau, \eta_n) \;=\; & w_r(\tau)\exp(j\pi\gamma\tau^2) \otimes_\tau \sum_{p=1}^{N_p(\eta_{nc})} \sum_{k=-N_k(\eta_{nc})/2}^{N_k(\eta_{nc})/2} \sigma(\eta_n, \rho_{np}, \theta_{nk}) \\ & \cdot \exp\left[-j2\pi f_c \left(R(\eta_{nc}, \rho_{np}) + \Delta R_1 + \Delta R_2\right)/c\right] \cdot \delta\left[\tau - R(\eta_n, \rho_{np}, \theta_{nk})/c\right] \end{aligned} \tag{14}$$

Provided that the subaperture time is very short, it is reasonable that scattering coefficient $\sigma(\eta_n, \rho_{np}, \theta_{nk})$ can be approximately substituted by $\sigma(\eta_{nc}, \rho_{np}, \theta_{nk})$. Further assume that the radar beam width is not very wide, so $\delta\left[\tau - 2R(\eta_n, \rho_{np}, \theta_{nk})/c\right]$ and $\delta\left[\tau - 2R(\eta_n, \rho_{np}, \theta_{n0})/c\right]$ are almost identical. Therefore, (14) becomes

$$\begin{aligned} s(\tau, \eta_n) \;\approx\; & w_r(\tau)\exp(j\pi\gamma\tau^2) \otimes_\tau \sum_{p=1}^{N_p(\eta_{nc})} \{\sigma(\eta_n, \rho_{np}) \\ & \cdot \exp\left[-j2\pi f_c \left(R(\eta_{nc}, \rho_{np}) + \Delta R_2\right)/c\right] \cdot \delta\left[\tau - R(\eta_n, \rho_{np}, \theta_{n0})/c\right]\} \end{aligned} \tag{15}$$

$\sigma(\eta_n, \rho_{np})$ is the scattering coefficient of the p-th equidistant elliptical ring domain at the position A_{η_n}, i.e.,

$$\sigma(\eta_n, \rho_{np}) = \sum_{k=-N_k(\eta_{nc})/2}^{N_k(\eta_{nc})/2} \sigma(\eta_{nc}, \rho_{np}, \theta_{nk}) \cdot \exp\left[-j2\pi f_c \Delta R_1/c\right] \tag{16}$$

r_{Mnp} is the range from the central pulse position $A_{\eta_{nc}}$ to the elliptical subscene $T(\rho_{np}, \theta_{n0})$, and the range from the stationary radar to the elliptical subscene $T(\rho_{np}, \theta_{n0})$ is r_{Snp}. r'_{Mnp} is the range from the current pulse position A_{η_n} to the elliptical subscene $T'(\rho_{np}, \theta_{nk})$, and the range from the stationary radar to the elliptical subscene $T'(\rho_{np}, \theta_{nk})$ is r'_{Snp}. Thus, we have

$$|A_{n\eta}T| + |BT| = \sqrt{r_{Mnp}^2 + d_{\eta_n}^2 + 2r_{Mnp}d_{\eta_n}\cos(\theta_{n0})} + r_{Snp} \approx r_{Mnp} + r_{Snp} + d_{\eta_n}\cos(\theta_{n0}) \tag{17}$$

In a similar way, the range $|A_{n\eta}T'| + |BT'|$ is approximated as

$$\left|A_{n\eta}T'\right| + \left|BT'\right| \approx r'_{Mnp} + r'_{Snp} + d_{\eta_n}\cos(\theta_{n0} + k\Delta\theta_n) \tag{18}$$

Then, the range difference ΔR_1 can be calculated by

$$\Delta R_1 \approx r'_{Mnp} + r'_{Snp} + d_{\eta_n}\cos(\theta_{n0} + k\Delta\theta_n) - (r_{Mnp} + r_{Snp} + d_{\eta_n}\cos(\theta_{n0})) \tag{19}$$

Under the assumption that radar beam width is not very wide, then $k\Delta\theta_n$ is usually small enough. Thus, $\cos(\theta_{n0}+k\Delta\theta_n)-\cos(\theta_{n0}) \approx -k\Delta\theta_n\sin(\theta_{n0})$ is reasonable. Besides $r_{Mnp}+r_{Snp} = r'_{Mnp}+r'_{Snp}$, then (19) is approximated as

$$\Delta R_1 \approx -d_{\eta_n}k\Delta\theta_n\sin(\theta_{n0}) \tag{20}$$

Therefore, (16) can be written as

$$\sigma(\eta_n, \rho_{np}) = \sum_{k=-N_k(\eta_{nc})/2}^{N_k(\eta_{nc})/2} \sigma(\eta_{nc}, \rho_{np}, \theta_{nk}) \cdot \exp\left[j2\pi f_c d_{\eta_n} k\Delta\theta_n \sin(\theta_{n0})/c\right] \tag{21}$$

If the scene angular sampling spacing is meet

$$\Delta\theta_n = c/(f_c d_{L_n}\sin(\theta_{n0})) \tag{22}$$

d_{L_n} is the range from the central pulse position $A_{\eta_{nc}}$ to edge pulse position, then (21) becomes

$$\sigma(\eta_n, \rho_{np}) = \sum_{k=-N_k(\eta_{nc})/2}^{N_k(\eta_{nc})/2} \sigma(\eta_{nc}, \rho_{np}, \theta_{nk}) \cdot \exp\left[j2\pi k d_{\eta_n}/d_{L_n}\right] \tag{23}$$

The size of the n-th subaperture is $2L_n$, and its index is $l_n = -L_n \cdots L_n$, then the discrete expression of (23) is

$$\sigma(l_n, \rho_{np}) = \sum_{k=-N_k(\eta_{nc})/2}^{N_k(\eta_{nc})/2} \sigma(\eta_{nc}, \rho_{np}, \theta_{nk}) \cdot \exp\left[j2\pi k W_{l_n}\right] \tag{24}$$

$W_{l_n} = d_{l_n}/d_{L_n} = l_n/L_n$, and d_{l_n} is the value of d_{η_n} at the l_n radar pulse position. Compared with the formula of the FFT, it is seen that (24) can be calculated by the FFT. The scene echo for the n-th subaperture is

$$\begin{aligned} s(\tau, \eta_n) \approx\ & w_r(\tau)\exp(j\pi\gamma\tau^2) \otimes_\tau \sum_{p=1}^{N_p(\eta_{nc})} \{\mathrm{FFT}\left[\sigma(\eta_{nc}, \rho_{np}, \theta_{nk})\right] \\ & \cdot \exp\left[-j2\pi f_c\left(R(\eta_{nc}, \rho_{np}) + \Delta R_2\right)/c\right] \cdot \delta\left[\tau - R(\eta_n, \rho_{np}, \theta_{n0})/c\right]\} \end{aligned} \tag{25}$$

Similarly, (25) can be performed by the FFT operation.

3.3. Implementation

According to the proposed RMS method, its implementation is given as follows:

(1) Set the simulation parameters and scene scattering coefficients; (2) Generate the transmitted signal and compute its FFT; (3) Divide the moving radar synthetic aperture into several subapertures; (4) Start the subaperture processing, separate the scene into several equidistant elliptical ring domain and elliptical subscenes; (5) Calculate the equivalent scattering coefficients of the elliptical subscenes at the subaperture central pulse. Based on this elliptical subscene scattering coefficients, calculate the equidistant elliptical rings' scattering coefficients for all the subaperture pulses using the FFT; (6) Calculate the system impulse response function and its FFT for all subaperture pulses; (7) Multiply the results of (2) and (6), and then transform their product into the time-domain using the IFFT and the obtain the subaperture pulse echo; (8) In terms of the subaperture order, repeat (4)–(7), and then the scene echo can be generated.

4. SIMULATION RESULTS

Simulation results are shown to verify the validity of the proposed RES method. Echo simulated by the TBT method is used as the referenced echo. To prove its correctness by the evaluation of imaging results, echoes simulated by different simulation methods are processed by the backprojection algorithm (BPA).

Simulation parameters are shown in Table 1. 81 scattering targets are located in the scene (200 m × 200 m, range × azimuth), and are arranged in 9 rows and 9 columns. Range and azimuth spacing between the adjacent scattering targets are 20.98 m and 22.44 m. Central target position is (1100 m, 0 m, 0 m). Scattering coefficients of all targets are assumed to be 1, and effects of the jamming, noise and multipath aren't considered.

Table 1: Simulation parameters of the OSBSAR system.

Center frequency	Signal bandwidth	Sampling frequency	Pulse duration	PRF	Azimuth beam width	Moving radar altitude (speed)	Stationary radar position
500 MHz	200 MHz	240 MHz	1 µs	100 Hz	10.2°	100 m(45 m/s)	(400, 0, 10) m

Figure 5 shows echoes simulated by the TBT and proposed RES methods. It is seen that the amplitude and phase of simulated echoes are very similar. Simulated echoes in Fig. 5 are processed by the BPA, and imaging results are shown in Fig. 6. It is found that the imaging results in Figs. 6(b) and 6(d) are very similar to that shown in Figs. 6(a) and 6(c), but their focusing qualities are slightly degraded due to the approximations in echo simulation. Processing time of the TBT and proposed RES methods are 20067.3 s and 1425.4 s, respectively. Compared with the TBT method, the simulation efficiency of the proposed method is improved about 14.1 times.

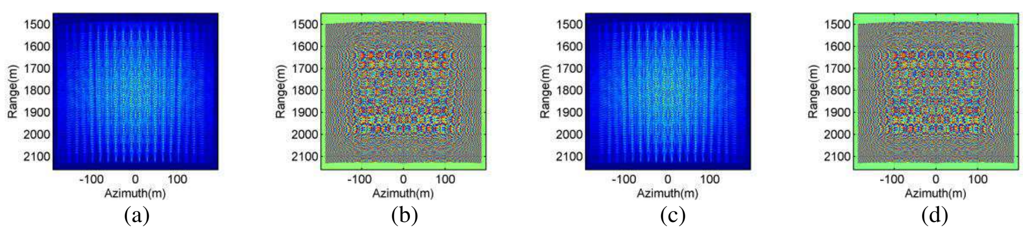

Figure 5: Scene echoes including 81 scattering targets. (a), (b) Amplitude and phase of the scene echo simulated by the TBT method; (c), (d) Amplitude and phase of the scene echo simulated by the proposed RES method.

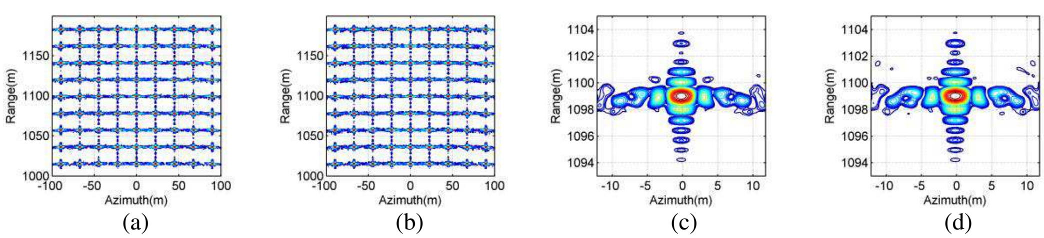

Figure 6: Imaging results. (a) Imaging result of the echo in Figs. 5(a)–(b); (b) Imaging result of the echo in Figs. 5(c)–(d); (c) Imaging result of the central target in Fig. 6(a); (d) Imaging result of the central target in Fig. 6(b).

5. CONCLUSION

This paper presents a rapid echo simulation method based on FFT and subaperture processing for OS-BSAR. The equivalent scatterer, subaperture processing and FFT operation can achieve great efficiency improvement in the OSBSAR echo simulation. The proposed RES method is verified by the simulation results, which has enriched the echo simulation method and will provide reliable echo source for the further OS-BSAR research.

ACKNOWLEDGMENT

This work was supported by the National Natural Science Foundation of China: Research on the key techniques of low frequency ultra wideband synthetic aperture radar interferometry (61201329) and Research Project of National University of Defense Technology (JC14-04-02).

REFERENCES

1. Xie, H. T., D. X. An, X. T. Huang, X. Y. Li, and Z. M. Zhou, "Fast factorised backprojection algorithm in elliptical polar coordinate for one-stationary bistatic very high frequency ultrahigh frequency ultra wideband synthetic aperture radar with arbitrary motion," *IET Radar Sonar Navig*, Vol. 8, No. 8, 946–956, Oct. 2014.
2. Xie, H. T., D. X. An, X. T. Huang, and Z. M. Zhou, "Fast time-domain imaging in elliptical polar coordinate for general bistatic VHF/UHF ultra-wideband SAR with arbitrary motion," *IEEE J. Sel. Topics Appl. Earth Observ.*, Vol. 8, No. 2, 879–895, Feb. 2015.
3. Henke, D., A. Barmettler, and E. Meier, "Bistatic experiment with the UWB-CARABAS sensor-first results and prospects of future applications," *Proc. IGARSS*, Capetown, South Africa, Jul. 2009, 234-237.
4. Franceschetti, G., M. Migliaccio, D. Riccio, and G. Schirinzi, "SARAS: A synthetic aperture radar (SAR) raw signal simulator," *IEEE Trans. Geosci. Remote Sens.*, Vol. 30, No. 1, 110–123, Jan. 1992.
5. Zhang, M., Y. W. Zhao, Y. Zhao, and H. Chen, "A bistatic synthetic aperture radar imagery simulation of maritime scene using the extended nonlinear chirp scaling algorithm," *IEEE Trans. Aerosp. Electron. Syst.*, Vol. 49, No. 3, 760–776, Jul. 2013.
6. Franceschetti, G., A. Iodice, A. Natale, and D. Riccio, "Bistatic SAR simulation time and frequency domain approaches," *Proc. DSP*, 1–7, Corfu, Greece, 2011.
7. Qiu, X. L., D. H. Hu, L. J. Zhou, and C. B. Ding, "A bistatic SAR raw data simulator based on inverse ω-k algorithm," *IEEE Trans. Geosci. Remote Sens.*, Vol. 48, No. 3, 1540–1547, Mar. 2010.
8. Wen, L. and T. Zeng, "A sub-aperture based SAR raw signal generation method," *Proc. IET International Radar Conference*, 89–92, Guilin, China, Jan. 2009.